International Journal of Current Research and Review
DOI: http://dx.doi.org/10.31782/IJCRR.2018.3645

Research Article

IJCRR
Section: General Science
Sci. Journal Impact Factor: 5.385 (2017)
ICV: 71.54 (2015)

Molecular Conformational Analysis, Vibrational Spectra, NBO, HOMO–LUMO and Molecular docking of Modafinil Based on Density Functional Theory

G. Bharathy[1]; Johanan Christian Prasana[2]; S. Muthu[3]

[1]Department of Applied Physics, Sri Venkateswara College of Engineering, Sriperumbudur, Tamil Nadu, India; [2]Department of Physics, Madras Christian College, Tambaram, Tamil Nadu, India; [3]Department of Physics, Arignar Anna Government Arts College, Cheyyar, Tamil Nadu, India.

ABSTRACT

Modafinil is a wakefulness-promoting agent used for treatment of disorders such as narcolepsy, Sleep disorders and excessive daytime sleepiness associated with obstructive sleep apnea. It has also been seen widespread psychostimulant used as a purported cognition-enhancing agent. IR and FT-Raman spectrum of Modafinil was analyzed. The vibrational wavenumber were computed using Density Functional Theory. The data obtained from wavenumber calculations are used to assign the vibrational bands obtained in the IR and Raman spectrum. The bond length and bond angles of the title compound are computed. NBO analysis, HOMO–LUMO, first and second order hyperpolarizability and molecular electrostatic potential results are also reported. PASS analysis of the Modafinil predicts sleep disorders treatment, activity with Pa (probability to be active) value of 0.822. Molecular docking studies exhibit the posing of ligand with the protein.

Key Words: DFT, HOMO energy, LUMO energy, Vibrational analysis, Hyperpolarisability, Docking

INTRODUCTION

The title compound Modafinil [(RS)-2-(diphenylmethyl) Sulfinyl] acetamide is an exclusive psychostimulant with a waking effect and is a special medicine that can only be prescribed to shift workers and patients suffering from narcolepsy. The normal half-life of modafinil in humans is between 12 to 15 hours. Modafinil consists of R- enantiomer and S - Enantiomer as a racemic compound and the waking effect of R-enantiomer has a longer duration. Moreover Armodafinil which is R-Enantiomer becomes commercial as waking drug. Pharmacological profile is notably different from traditional psychostimulants such as methyphenidate as cocaine. Modafinil is less related to side effects such as excess locomotor activities. The Orexin neutrons may be activated by Modafinil. The Orexin neutrons are found exclusively in the lateral hypothalamus & hypothalamic area projects to the entire central nervous system. However the waking mechanism is yet to be fully elucidated. Modafinil increases histamine release significantly in the anterior hypothalamus. It is well known that the terminal amide group is responsible for biological activity. [1].The main objective of this work is to adapt different Spectroscopic techniques and Quantum chemical calculation on title compound there by unveiling its interesting chemical bonding and electronic behaviour.

MATERIALS AND METHODS

The optimized molecular structure, molecular electrostatic potential, and vibrational spectra of the title compound were calculated by the density functional theory method with 6-31G (d,p) basis sets. Density functional theory was proven to be extremely useful in treating electronic structure of molecules [2-4]. The basis set 6-31G (d,p) was used as an effective and economical level to study fairly large organic molecules. Based on the points, the density functional three-

Corresponding Author:
G. Bharathy, Department of Applied Physics, Sri Venkateswara College of Engineering, Sriperumbudur, Tamil Nadu, India.
Email: gbharathy@svce.ac.in

ISSN: 2231-2196 (Print) **ISSN:** 0975-5241 (Online)
Received: 18.07.2018 **Revised:** 16.08.2018 **Accepted:** 19.10.2018

parameter hybrid model (B3LYP) at the 6-31G (d, p) basis set level was adopted to calculate the properties of the studied molecule in the present work. All the calculations were performed using the Gaussian 03W [5] program package with the default convergence criteria, without any constraint on the geometry. The geometries of the title compound have been first optimized with full relaxation on the potential energy surfaces at B3LYP/6-31G (d, p) level and resultant geometries have been re-optimized for further calculation. Scaling of the field was performed according to the quantum mechanical procedure, using selectively scaling since the program is run in its gaseous phase. The scale factor calculation and characterization of the normal modes using potential energy distribution was done by using VEDA [6] program. The properties, such as HOMO and LUMO energies, were determined by time-dependent density functional theory approaching. The hyperpolarisability values of the molecule have been computed and tabulated [7-9] and Gauss view [10] program to confirm HOMO and LUMO plot.

RESULTS AND DISCUSSION

Vibrational Analysis

The title compound consists of 34 atoms and has 96 normal modes of vibration. Modafinil has 33 stretching modes, 36 bending modes and 27 torsional modes of vibration. The observed theoretically scaled frequencies along with their PED are presented in Table 3. The functional groups present in the molecule were identified and a satisfactory vibrational band assignment has been made for the fundamental modes of vibration by observing the position, shape and intensity of the bands.

The Aromatic C–H ring stretching vibrations are normally found in the region 3100–3000 cm^{-1} [11]. However these bands are rarely used because they overlap with one another resulting in stronger absorption in this region. For the title compound the C-H stretching were observed from 3225 cm^{-1} to 3077 cm^{-1}. Scaled vibrations assigned to the C–H stretching with PED contribution of 92% .The Carbon–Carbon stretching modes for the title compound is assigned at the frequencies 1666,1660,1644,1641,1632cm^{-1} HNC bending, HCC bending, HCH,CSC bending, OSC bending, CCC bending are observed at the frequencies 1468Cm^{-1},1235-1413Cm^{-1},1384 Cm^{-1}, 1085 Cm^{-1},1033 Cm^{-1} respectively. The frequency assignment table clearly depicts the HCCC torsion, HOCC torsion, HNCC torsion CCCC torsion and CCNC torsion at various frequencies. The identification of CN vibration is difficult since mixing of vibration is possible in this region. Silverstein et al [12] assigned CN stretching absorption in the region 1266-1382Cm^{-1} for aromatic amines. In the title compound CN stretching is observed at the frequencies1375-1364Cm^{-1}. Most of the modes are not pure, but it also contains significant contribution from other modes too.

Geometrical Parameters

The numbering system adopted in the molecular structure of the title compound is shown in Fig. 3. The optimized geometrical parameter calculated by DFT/B3LYP with 6-31G (d,p) basis set is listed in Table 1. In this title compound the C-S bond length is in computed to be 1.859Å while reported value is about 1.861Å [13]. The C-N bond length for the title compound is found to be 1.359Å which is in good agreement with literature [14]. Modafinil has a chiral centre at the sulphur atom. The bond length and bond angles are given in the table.1

Frontier Molecular Orbital Analysis

Knowledge of the highest occupied molecular orbital (HOMO) and lowest unoccupied molecular orbital (LUMO) and their properties such as their energy is very useful to gauge the chemical reactivity of the molecule. The ability of the molecule to donate an electron is associated with the HOMO and the characteristic of the LUMO is associated with the molecule's electron affinity. The HOMO and LUMO energies are very useful for physicists and chemists and are very important terms in quantum chemistry [15, 16]. The absorption of energies corresponds to the transition from the ground state to the first excited state and is mainly described by an electron excitation from the HOMO to the LUMO. The pictorial representation of the HOMO and the LUMO in the gaseous phase is shown in Fig.5. The HOMO lies at -6.3169 eV whereas the LUMO is located at -0.87159 eV and the frontier orbital energy gap is 5.445313 eV. The lower the energy gap the more easily are the electrons excited from the ground to the excited state. The energy gap explains the transference of charge and hence its interaction within the molecule and is useful in determining molecular electrical transport properties [17]. Both the HOMO and LUMO orbital are the main orbitals which decide the chemical stability of the molecule. By using the HOMO and LUMO energy values, the global chemical reactivity descriptors such as hardness, chemical potential, electro-negativity and electrophilicity index as well as local reactivity can be defined [18-22]. Pauling introduced the concept of electro-negativity as the power of an atom in a molecule to attract electrons to it. Hardness (η), chemical potential (μ) and electro-negativity (χ) are defined using Koopman's theorem as $\eta = (I- A)/2 =$ 2.7226 eV, $\mu = -(I + A)/2 =$-3.59424 eV and $\chi = (I + A)/2 =$ 3.59424 eV, where A and I are the ionization potential and electron affinity of the molecule. $I = -E_{HOMO} =$6.3169 eV and $A = E_{LUMO} =$-0.87159 eV. The stability of the molecule is related to hardness, which means that the molecule with a lower energy gap shows higher reactivity [23]. Parr et al. [18] have defined a descriptor to quantify the global electro-

philic power of the molecule as the electrophilicity index = $\mu^2/2\eta$ =2.372424 eV.

ELECTROSTATIC POTENTIAL

The electrostatic potential is the potential energy felt by a positive "test" charge at a particular point in space. If the ESP is negative, this is a region of stability for the positive test charge. Conversely, if the ESP is positive, this is a region of relative instability for the positive test charge. Thus, an ESP-mapped density surface can be used to show regions of a molecule that might be more favourable to nucleophilic or electrophilic attack, making these types of surfaces useful for qualitative interpretations of chemical reactivity. The ESP-mapped density surface shows "where" the frontier electron density for the molecule is greatest (or least) relative to the nuclei. The colours are the value of the ESP at the points on the electron density surface. The colour map is given on the left. Note the large red region around the oxygen-end of the molecule. One can find enhanced electron density here. The red colour indicates the most negative regions of the electrostatic potential where a positive test charge would have favourable interaction energy. The hydrogen-end of the molecule, with the magenta colour, shows regions of relatively unfavourable energy for the ESP. Potential increases in the order blue to red. Such mapped electrostatic potential surfaces have been plotted for title molecule in B3LYP/6-31G (d, p) basis set using the software Argus Lab [Fig 4]

NBO Analysis

The natural bond orbital (NBO) calculations were performed using Gaussian 03 package in order to understand various second order interaction between the filled orbital of one system and vacant orbital of another subsystem, which is a measure of delocalization or hyper- conjugation. The hyper-conjugative interaction energy was deduced from second order perturbation approach [24]. For each donor (i) and acceptor (j) the stabilization energy (E2) associated with the delocalization i→j is determined as $E(2) = \Delta E_{ij} = q_i \frac{(F_{ij})^2}{(E_j - E_i)}$

Where q_i→donor orbital occupancy, E_i,E_j→diagonal elements and F_{ij}→off diagonal NBO Fock matrix elements.In NBO analysis large value of E(2) shows the intensive interaction between donors and acceptors. The possible interactions are tabulated in Table 2.The second -order perturbation theory analysis of Fock matrix in NBO basis shows strong inter-molecular hyper conjugative interactions are formed by orbital which results in intra-molecular charge transfer causing stabilization of the system. The interactions π^*(C16-C17) → π^* (C14-C15) and π^*(C18-C19) having the stabilization energy 74.15KJmol^{-1} and 86.99KJmol^{-1}LP (2) O3→ σ^*(C1-C2) and σ^*(C1-N4) having the stabilization energy 11.15KJmol^{-1} and 13.46KJmol^{-1} are responsible for hyper conjugation. The hyper-conjugative interaction energy was deduced from the second-order perturbation approach. This gives an idea about electron density between occupied Lewis-type (bond) NBO orbital and unoccupied (anti-bond) non-Lewis NBO orbital corresponds to a stabilizing donor–acceptor interaction.

Docking

Docking is a tool to predict the preferred orientation of a molecule which bound to each other to form stable complex. The preferred orientations of a molecule may be used to predict the binding affinity between two molecules. Docking is frequently used to predict the binding orientations of small molecules (drug) to protein targets which in turn predict the affinity and activity of the small molecule. The receiving molecule that primarily binds to a small molecule or another protein or a nucleic acid is called a receptor. A molecule that forms the complementary partner in the docking process is called a ligand (Bharatam et al., 2007).

PASS (Prediction of Activity Spectra) [25] is an online structure activity relationship (SAR) tool which predicts biological activity based on the structure of a molecule. PASS analysis of the modafinil predicts sleep disorders treatment, activity with Pa (probability to be active) value of 0.822. Molecular docking simulations were done on Auto Dock Vina software [26]. Auto Dock Tools (ADT) graphical user interface was used to add polar hydrogen and atomic charges by Kollman method. Water molecules and co-crystallised ligands were removed and the modafinil was prepared for docking by minimizing its energy at B3LYP/6-31G(d,p) level of theory. ADT was employed to add partial charges by Geistenger method and to define torsions and rotatable bonds. The active site of the enzyme was defined in a manner so as to include residues of the active site within the grid. Lamarckian Genetic Algorithm (LGA) available in Auto Dock Vina was employed for docking. The docking protocol has been tested by removing co-crystallized inhibitor from the protein and then docking it at the same site. To evaluate the quality of docking results, the common way is to calculate the Root Mean Square Deviation (RMSD) between the docked pose and the known crystal structure conformation. RMSD values up to 2 Å are considered as reliable for a docking protocol [27]. The docking protocol employed predicts similar conformation with RMSD value well within the reliable range (Fig. 6). The ligand, binds at the active site of the protein by weak non-covalent interactions (H-bonds and alkyl-p interactions). The ligand molecule is held at the active site of substrate by strong H-bonds with amino acids. These results draw us to the conclusion that the compound exhibit Psychostimulant activity. However, biological tests need to be done to validate the computational predictions.

CONCLUSIONS

FT-IR and Raman spectra of the title compound were studied. The geometrical parameters were calculated using DFT method and conformers were studied. The stability of the molecule arising from the idea on electron occupancy has been analysed using NBO analysis. The energy band gap is calculated by using HOMO and LUMO analysis which explained the transfer of charges within the molecule. Docking study shows good hydrophobic nature of the title compound and it may act as narcolepsy inhibitor.

ACKNOWLEDGEMENTS

The authors express their sincere thanks to Head of the Department, Department of Applied Physics, Sri Venkateswara College of Engineering, Sriperumbudur for extending the support this research work.

REFERENCES

1. Wong Y.N., Simcoe D., Hartman L.N., Laughton W.B., King S.P., McCormick G.C., Grebow P.E., J. Clin. Pharmacol., 39, 30-40 (1999)
2. F. Sim, A.S. Amant, I. Papai, and D.R. Salahub, Gaussian density functional calculations o n hydrogen-bonded systems, J. Am. Chem. Soc. 114 (1992), pp. 4391–4400.
3. V. Krishnakumar, V. Balachandran and T. Chithambarathanu, Density functional theory study of the FT-IR spectra of phthalimide and N-bromophthalimide, Spectrochim. Acta A 62 (2005),pp. 918–925.
4. L. Fan and T. Ziegler, Application of density functional theory to infrared absorption intensity calculations on transition-metal carbonyls, J. Phys. Chem. 96 (1992), pp. 6937–6941.
5. M.J. Frisch, G.W. Trucks, H.B. Schlegel, G.E. Suzerain, M.A. Robb, J.R. Cheeseman, Jr., J.A. Montgomery, T. Vreven, K.N. Kudin, J.C. Burant, J.M. Millam, S.S. Iyengar, J. Tomasi, V. Barone, B. Mennucci, M. Cossi, G. Scalmani, N. Rega, G.A. Petersson, H. Nakatsuji, M. Hada, M. Ehara, K. Toyota, R. Fukuda, J. Hasegawa, M. Ishida, T. Nakajima, Y. Honda, O. Kitao, H. Nakai, M. Klene, X. Li, J.E. Knox, H.P. Hratchian, J.B. Cross, V. Bakken, C. Adamo, J. Jaramillo, R. Gomperts, R.E. Stratmann, O. Yazyev, A.J. Austin, R. Cammi, C. Pomelli, J.W. Ochterski, P.Y. Ayala, K. Morokuma, G.A. Voth, P. Salvador, J.J. Dannenberg, V.G. Zakrzewski, S. Dapprich, A.D. Daniels, M.C. Strain,O. Farkas, D.K. Malick, A.D. Rabuck, K. Raghavachari, J.B. Foresman, J.V. Ortiz, Q. Cui, A.G. Baboul, S. Clifford, J. Cioslowski, B. Stefanov, G. Liu, A. Liashenko, P. Piskorz, I. Komaromi, R.L. Martin, D.J. Fox, T. Keith, M.A. Al-Laham, C.Y. Peng, A. Nanayakkara, M. Challacombe, P.M.W. Gill, B. Johnson, W. Chen, M.W. Wong, C. Gonzalez, and J. A. Pople, Gaussian 03, Revision A.I, Gaussian, Inc, Pittsburgh, PA, 2003.
6. M.H. Jamroz, Vibrational Energy Distribution Analysis, VEDA 4, computer program, Poland, 2004.
7. P.M.W. Gill, B.G. Johnson, J.A. Pople, M.J. Frisch, Chem. Phys. Lett. 197 (1992)499.
8. Venkatesan , P , Thamotharan , S , Ilangovan , A , Liang , H & Sundius , T Spectrochimica Acta Part A: Molecular and Biomolecular Spectroscopy,153(2016) 625-636
9. M. Karabacak, M. Kurt, A. Atac, J. Phys. Org. Chem. 22 (2009) 321.
10. R.I. Dennington, T. Keith, J. Millam, GaussView, Version 5.0.8, Semichem. Inc.,Shawnee Mission, KS, 2008.
11. M. Karabacak, M. Cinar, M. Kurt, J. Mol. Struct. 968 (2010) 108.
12. R.M. Silverstein, G.C.Bassler, T,C. Morril, Spectrometric Identification of Organic compounds, fifth de., John Wiley and Sons Inc., Singapore, 1991.
13. J. Olsen, P. Jorgensen, J.Chem.Phys.82 (1985) 3235-3264.
14. R. Shanmugam, D. Sathyanarayana, Spectrochim. Acta 40 (1984) 764-773.
15. K. Fukui, Science 218 (1982) 474–754.
16. S. Gunasekaran, R.A. Balaji, S. Kumaresan, G. Anand, S. Srinivasan, Can. J. Anal. Sci. Spectrosc. 53 (2008) 149–162.
17. J. Daisy Magdaline, T. Chithabarathanu, J. Appl. Chem.8(2015) 06-14.
18. R.G. Parr, L. Szentpaly, S. Liu, J. Am. Chem. Soc. 121 (1999) 1922–1924.
19. P.K. Chattaraj, B. Maiti, U. Sarkar, J. Phys. Chem. A 107 (2003) 4973–4975.
20. R.G. Parr, R.A. Donnelly, M. Ley, W.E. Palke, J. Chem. Phys. 68 (1978) 3801–3807.
21. R.G. Parr, R.G. Pearson, J. Am. Chem. Soc. 105 (1983) 7512–7516.
22. R.G. Parr, P.K. Chattaraj, J. Am. Chem. Soc. 113 (1991) 1854–1855.
23. S. Muthu, N. R. Sheela, S. Sampath Krishnan, Molecular Simulation 37(2011) 1276-1288
24. E.D. Glendening, A.E. Reed, J.E. Carpenter, F. Weihhold, NBO Version 3.1. Theoretical Chemistry Institute and Department of Chemistry, University of Wisconsin, Madison, 1988.
25. A. Lagunin, A. Stepanchikova, D. Filimonov, V. Poroikov, Bioinformatics 16 (2000) 747–748.
26. O. Trott, A.J. Olson, J. Comput. Chem. 31 (2010) 455–461.
27. B. Kramer, M. Rarey, T. Lengauer, Proteins: Struct. Funct. Genet. 37 (1999) 228–241.

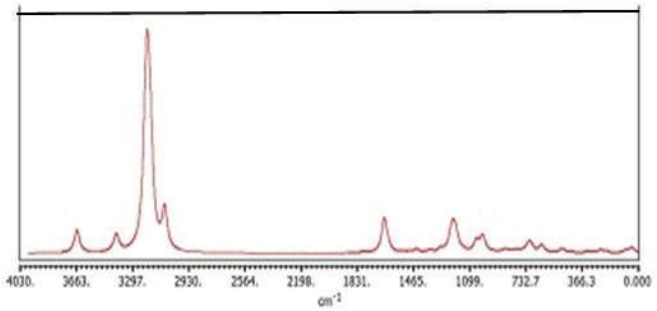

Figure 1: FT Raman Spectrum of Modafinil.

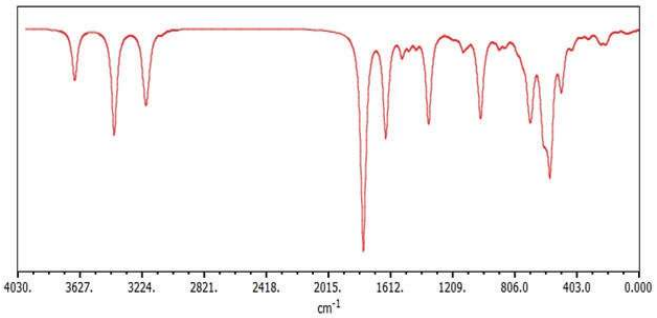

Figure 2: IR spectrum of Modafinil.

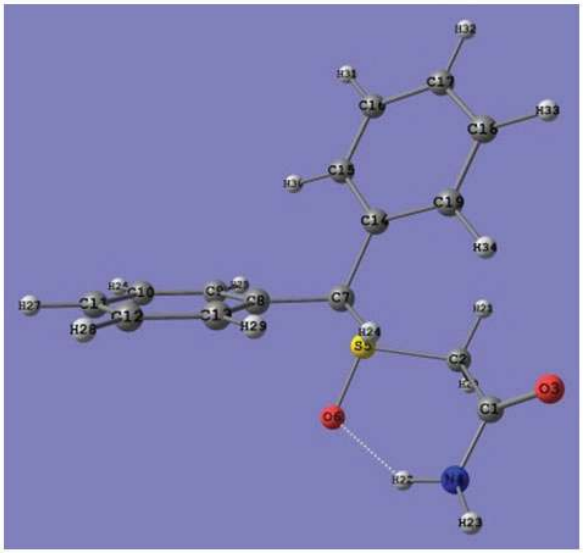

Figure 3: Optimized geometry of Modafinil.

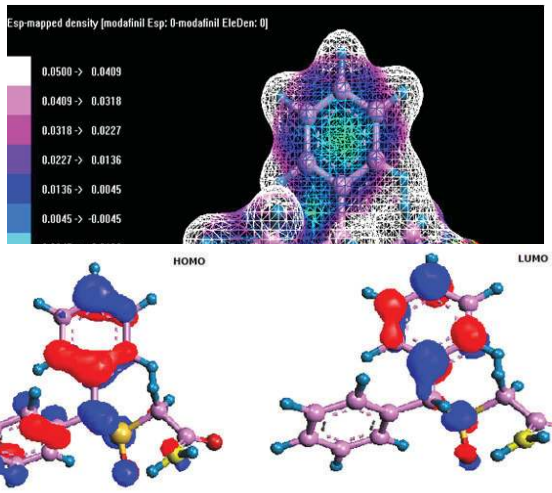

Figure 5: HOMO and LUMO plots of Modafinil.

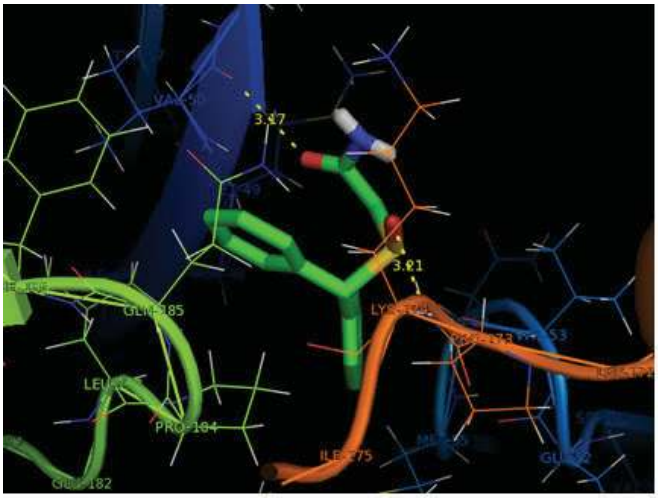

Figure 6: Docking of Title compound.

Table 1: Optimized geometrical parameters (B3LYP/6-31G) of Modafinil, atom labelling according to Fig. 3.

Bond lengths (Å)		Bond angles (°)		Bond angles (°)	
C1-C2	1.532	C2-C1-O3	121.2	C11-C12-H28	120.2
C1-O3	1.226	C2-C1-N4	114.3	C13-C12-H28	119.7
C1-N4	1.359	C1-C2-S5	114.6	C12-C13-H29	119.7
C2-S5	1.859	C1-C2-H20	110.6	C15-C14-C19	118.6
C2-H20	1.094	C1-C2-H21	109.7	C14-C15-C16	120.6
C2-H21	1.089	O3-C1-N4	124.5	C14-C15-H30	119.9
N4-H22	1.022	C1-N4-H22	118.1	C14-C19-C18	120.6
N4-H23)	1.01	C1-N4-H23	116.3	C14-C19-H34	119.7

Table 1: *(Continued)*

Bond lengths (Å)		Bond angles (°)		Bond angles (°)	
S5-O6	1.525	S5-C2-H20	103.3	C16-C15-H30	119.4
C7-C8	1.516	S5-C2-H21	108.7	C15-C16-C17	120.3
C7-C14	1.517	C2-S5-O6	105.6	C15-C16-H31	119.6
C7-H24	1.093	H20-C2-H21	109.7	C17-C16-H31	120.1
C8-C9	1.402	H22-N4-H23	119.6	C16-C17-C18	119.6
C8-C13	1.401	N4-H22-O6	141.2	C16-C17-H32	120.2
C9-C10	1.395	S5-O6-H22	102.3	C18-C17-H32	120.3
C9-H25	1.086	C8-C7-C14	116.2	C17-C18-C19	120.3
C10-C11	1.395	C8-C7-H24	108.3	C17-C18-H33	120.2
C10-H26	1.086	C7-C8-C9	123.1	C19-C18-H33	119.5
C11-C12	1.395	C7-C8-C13	118.4	C18-C19-H34	119.6
C11-H27	1.086	C14-C7-H24	109.1		
C12-C13	1.394	C7-C14-C15	121.9		
C12-H28	1.086	C7-C14-C19	119.4		
C13-H29	1.087	C9-C8-C13	118.5		
C14-C15	1.403	C8-C9-C10	120.7		
C14-C19	1.405	C8-C9-H25	120.3		
C15-C16	1.395	C8-C13-C12	120.9		
C15-H30	1.084	C8-C13-H29	119.4		
C16-C17	1.395	C10-C9-H25	119		
C16-H31	1.086	C9-C10-C11	120.3		
C17-C18)	1.396	C9-C10-H26	119.6		
C17-H32	1.086	C11-C10-H26	120.1		
C18-C19	1.395	C10-C11-C12	119.5		
C18-H33	1.086	C10-C11-H27	120.2		
C19-H34	1.087	C12-C11-H27	120.2		
O6-H22	1.93	C11-C12-C13	120.1		

Table 2: NBO results showing the formation of Lewis and non-Lewis orbitals

Donor (i)	Type	ED/e	EDA%	EDB%	NBO	S%	P%
C 1 - C 2	σ	1.9816	46.82	53.18	0.6843(sp1.82)C+0.7282(sp2.97)C	35.47	64.48
						27.07	72.88
C 1 - O 3	σ	1.99698	33.68	66.32	0.5803(sp2.21)C+0.8144(3sp1.33)C	31.13	68.75
						42.71	56.94
C 1 - O 3	π	1.98046	34.18	65.82	0.5846(sp77.9)C+0.8113(sp93.66)O	1.27	98.58
						1.05	98.61
C 1 - N 4	σ	1.9946	38.83	61.17	0.6231(sp2.12)C+0.7821(sp1.67)C	32	67.88
						37.38	62.58
C 2 - S 5	σ	1.9636	54.5	45.5	0.7382(sp3.86)C+0.6746(sp5.61)C	20.58	79.37
						14.97	83.96
C 2 - H 20	σ	1.9819	63.94	36.06	0.7996(sp3.02)C+0.6005(sp)H	24.89	75.07
						99.95	0.05
C 2 - H 21	σ	1.8918	62.92	37.08	0.7932(sp2.65)C+0.6089(sp)H	27.4	72.57

						99.97	0.03
N 4 - H 22	σ	1.97792	72.85	27.15	0.8535(sp2.06)N+0.5210(sp)H	32.72	67.25
						99.9	0
N 4 -H 23	σ	1.98074	71.08	28.92	0.8431(sp2.95)N+0.5378(sp)H	29.82	70.16
						99.91	0.09
S 5 - O 6	σ	1.98904	34.05	65.95	0.5835(sp4.36)S+0.8121(sp3.15)o	18.45	80.36
						23.98	75.5
S 5 - C 7	σ	1.96527	44.15	55.85	0.6644(sp5.49)S+0.7473(sp4.00)o	15.22	83.65
						19.99	79.96
C 7 - C 8	σ	1.9738	51.11	48.89	0.7149(sp2.54)C+0.6992(sp2.20)C	28.22	71.74
						31.25	68.71
C 7 - C 14	σ	1.96611	50.67	49.33	0.7119(sp2.61)C+0.7023(sp2.21)C	27.71	72.25
						31.16	68.8
C 8 - C 9	σ	1.97622	51.36	48.64	0.7167(sp1.90)C+0.6974(sp1.91)C	34.43	65.53
						34.39	65.57
C 8 - C 9	π	1.6679	50.85	49.15	0.7131(sp99.99)C+0.7010(sp1.00)C	0.02	99.95
						0.01	99.95
C 9 - H 25	σ	1.97506	62.84	37.16	0.7927(sp2.29)C+0.6096(sp)H	30.41	69.54
						99.95	0.05
C 10- C 11	σ	1.98279	49.98	50.02	0.7070(sp1.86)C+0.7072(sp1.85)C	34.95	65.01
						35.05	64.91
C 10- C 11	π	1.66546	49.65	50.35	0.7046(sp1.00)C+0.7096(sp)C	0	99.96
						0	99.96
C 14 - C 15	σ	1.9743	51.58	48.42	0.7182(sp1.85)C+0.6958(sp1.94)C	35.08	64.88
						34.03	65.93
C 14 - C 15	π	1.65369	51.6	48.4	0.7184(sp99.99)C+0.6957(sp1.00)C	0.02	99.96
						0.01	99.95
C 16 - C 17	σ	1.98333	49.99	50.01	0.7070(sp1.87)C+0.7075(sp1.85)H	34.81	65.15
						35.08	64.88
C 16 - C 17	π	1.64954	49.65	50.35	0.7046(sp1.00)C+0.7096(sp1.00)C	0	99.96
						0	99.96
C 1 - O 3	σ*	0.04896	66.32	33.68	0.8144(sp2.21)C-0.5803(sp1.33)O	31.13	68.75
						42.71	56.94
C 1 - O 3	π*	0.15263	65.82	34.18	0.8113(sp77.90)C-0.5846(sp)O	1.27	98.58
						1.05	98.61
C 1 - N 4	σ*	0.0688	61.17	38.83	0.7821(sp2.12)C-0.6231(sp1.67)N	36.6	63.36
						36.97	62.98
C 2 - S 5	σ*	0.12461	45.5	54.5	0.6746(sp3.86)C-0.7382(sp5.61)S	0	99.95
						0	99.98
C 2 - H 20	σ*	0.01461	36.06	63.94	0.6005(sp3.02)C-0.7996(sp0.00)H	24.89	75.07
						99.95	0.05
C 2 - H 21	σ*	0.12293	37.08	62.92	0.6089(sp2.65)C-0.7932(sp1.91)H	27.4	72.57
						99.97	0
N 4 -H 22	σ*	0.02907	27.15	72.85	0.5210(sp2.06)N-0.8535(sp0.00)H	32.72	67.25
						99.9	0.1

N 4 -H 23	σ*	0.01117	28.92	71.08	0.5378(sp2.35)N-0.8431(sp0.00)H	29.82	70.16
						99.91	0.09
S 5 - O 6	σ*	0.02955	65.95	34.05	0.8121(sp4.36)S-0.5835(sp3.15)O	18.45	80.36
						23.98	75.5
S 5- C 7	σ*	0.13612	55.85	44.15	0.7473(sp5.49)S-0.6644(sp4.00)C	15.22	83.65
						19.99	79.96
C 7 - C 8	σ*	0.0291	48.89	51.11	0.6992(sp2.54)C-0.7149(sp1.81)C	28.22	71.74
						31.25	68.71
O 3	LP (1)	1.976			(sp0.78)O	56.18	43.77
O 3	LP (2)	1.87205			(sp99.99)O	0.02	99.75
N 4	LP (1)	1.85779			(sp1.00)N	0.01	99.98
S 5	LP (1)	1.96783			(sp0.92)S	52.08	47.9
O 6	LP (1)	1.98432			(sp0.32)O	75.88	24.1
O 6	LP (2)	1.87475			(sp99.99)O	0.15	99.56
O 6	LP (3)	1.80392			(sp99.99)O	0.01	99.67

Table 3: The calculated and vibrational wavenumber, measured IR and Raman Band positions (Cm^{-1}) and assignment of the title compound

Mode no	Calculated Frequency Cm^{-1}	FTIR		Raman		Vibrational assignments (PED%)
		Relative[a]	Absolute[b]	Relative[a]	Absolute[b]	
1	3669.87	63.9783	23.1	92.9713	32.6	ν NH(67)+ ϕ HNH(19)
2	3400.78	133.044	48	71.1371	25	ν NH(63)+ ϕ HNC(20)
3	3225.04	9.2878	3.35	190.1004	66.7	ν CH(39)+ τ HCCC(11)
4	3210.83	18.2383	6.58	285.5431	100	ν CH(48)
5	3206.67	23.4086	8.45	192.694	67.6	ν CH(68)
6	3200.28	23.4135	8.45	51.5106	18.1	ν CH(77)
7	3191.16	9.8899	3.57	45.5214	16	ν CH(27)+ ϕ HCH(18)
8	3189.73	14.5243	5.24	81.523	28.6	ν CH(43)
9	3185.4	6.0797	2.19	128.1917	45	ν CH(23)+ ϕ HCH(16)
10	3178.56	1.4987	0.54	92.8999	32.6	ν CH(45)+ τ HCCC(11)
11	3175.74	0.4193	0.15	43.9722	15.4	ν CH(51)
12	3165.34	0.5714	0.21	17.5395	6.15	ν CH(36)+ ϕ HCH(11)
13	3149.91	5.3218	1.92	18.2276	6.4	ν CH(47)
14	3096.84	3.0591	1.1	27.6306	9.69	ν CH(92)
15	3077.34	0.666	0.24	135.2384	47.5	ν CH(28)+ ϕ HCC(31)+ τ HCCN(14)
16	1775.69	277.424	100	6.0426	2.12	NCCS (17)+ γOCNC (58)
17	1666.28	2.2305	0.81	65.287	22.9	ν CC (28)
18	1660.87	2.9758	1.07	66.9845	23.5	ν CC (26)
19	1644.57	119.315	43.1	6.6925	2.35	ν CC (15)
20	1641.63	4.2569	1.54	9.6333	3.38	ν CC (29)
21	1632.84	4.2952	1.55	6.4867	2.28	HNC(15)+ ϕ HNH(25)
22	1540.23	7.6055	2.75	3.288	1.15	HCC(61)
23	1534.76	19.0308	6.87	2.1934	0.77	HCC(53)
24	1500.06	2.6395	0.95	2.0213	0.71	HCC(39)
25	1496.84	12.2346	4.42	1.6923	0.59	ν CC(21)+ ϕ HCC(35)

Mode no	Calculated Frequency Cm^{-1}	FTIR		Raman		Vibrational assignments (PED%)
		Relative[a]	Absolute[b]	Relative[a]	Absolute[b]	
26	1448.85	12.9437	4.67	15.0579	5.28	ν CH(65)+ ϕ HCH(13)
27	1392.69	2.0304	0.73	0.9929	0.35	HCC(24)+ τ HCCC(12)
28	1375.99	10.713	3.87	1.3928	0.49	ν NC(12)
29	1367.59	103.461	37.4	3.0698	1.08	ν CC(30)
30	1364.28	1.2943	0.47	1.6562	0.58	ν NC(16)+ ϕ HCC(11)
31	1344.72	0.4885	0.18	4.6148	1.62	ν NC(16)+ ϕ HCC(11)
32	1290.72	0.7006	0.25	15.8998	5.58	HCCC(13)
33	1254.57	1.5344	0.55	2.6036	0.91	HCH(12)+ τ HCCN(64)
34	1223.57	0.3261	0.12	31.5693	11.1	ν CC(22)+ τ HCCC(28)
35	1214.12	1.4948	0.54	12.3078	4.32	HCC(35)+ τ HCCC(13)
36	1210.94	1.4418	0.52	17.2351	6.05	HCC(37)
37	1206	2.7452	0.99	59.9409	21	HCC(14)
38	1197.65	0.3708	0.13	25.3838	8.91	ν CC(20)
39	1188.52	0.0496	0.02	7.865	2.76	HCC(11)
40	1185.86	0.4142	0.15	12.7788	4.48	HCC(24)
41	1184.4	2.8273	1.02	10.6882	3.75	HCC(24)
42	1151.86	19.4077	7.01	6.596	2.31	HCC(28)+ τ HCCN(12)
43	1117.71	7.9662	2.88	0.782	0.27	ν CC(14)
44	1098.17	0.6794	0.25	0.2384	0.08	ν CC(13)
45	1056.54	4.4013	1.59	8.9056	3.12	ν CC(27)+ τ CCCC(11)
46	1054.16	1.0354	0.37	36.5508	12.8	ν CC (23)
47	1033.21	103.027	37.2	5.1084	1.79	ν SO (76)
48	1016.92	4.4831	1.62	48.2308	16.9	CCC(16)
49	1010.97	1.648	0.59	11.5639	4.06	CCC (14)
50	1006.71	1.0184	0.37	1.8761	0.66	HCCC(26)
51	1001.33	0.0138	0	0.2359	0.08	HCC(13)+ τ HCCC(45)
52	985.05	2.3142	0.84	2.1534	0.76	ν CH(10)+ τ HCCC(37)
53	976.25	0.0457	0.02	0.4645	0.16	HCCC(54)
54	949.52	3.3285	1.2	2.4667	0.87	HCCC(39)
55	935.75	0.388	0.14	1.2969	0.46	HCCC(52)
56	928.19	15.0807	5.44	4.2297	1.48	τ NCCS(15)
57	898.6	3.6944	1.33	3.2552	1.14	ν CC (16)+ τ HCCN(10)
58	875.59	5.7316	2.07	2.2979	0.81	τ HCCC (32)
59	863.37	4.6289	1.67	4.1054	1.44	HCCC (32)
60	839.77	0.0492	0.02	3.7343	1.31	-
61	828.91	2.6454	0.96	8.1651	2.86	-
62	797.09	13.8652	5.01	9.6868	3.4	HCCC (10)+ γ CCCC (10)
63	765.65	13.9308	5.03	3.0261	1.06	-
64	735.31	7.6927	2.78	3.5046	1.23	CCCC(11)
65	721.46	20.3902	7.36	19.4241	6.82	HNCC(17)+ τ CCCC(11)
66	712.55	26.3029	9.5	1.8622	0.65	HNCC(11)+ τ CCCC(10)
67	699.68	19.5613	7.06	13.6593	4.79	HNCC(11)+ τ CCCC(24)
68	669.21	54.1917	19.6	19.7866	6.94	ν SC (55)

Mode no	Calculated Frequency Cm^{-1}	FTIR		Raman		Vibrational assignments (PED%)
		Relative[a]	Absolute[b]	Relative[a]	Absolute[b]	
69	632.59	11.0867	4	9.7969	3.44	CCC (25)
70	631.24	4.4722	1.61	8.5912	3.01	CCC (10)+ τ CCCC(12)
71	618.03	3.2815	1.18	9.1652	3.22	CCC(13)
72	606.47	75.7278	27.3	5.0856	1.78	HNCC (16)
73	589.11	47.7589	17.2	2.0734	0.73	HNCC (15)
74	557.42	147.299	53.2	0.5351	0.19	ν NC(12)+ ν CC (12)+ τ HNCC(23)
75	503.97	58.4307	21.1	4.9282	1.73	OCN(16)+ γ CCCC(13)
76	492.61	4.5291	1.64	11.0897	3.89	νSC (17)
77	486.76	0.471	0.17	3.7895	1.33	CCCC (11)
78	427.88	15.2089	5.49	2.6571	0.93	OSC (34)
79	417.81	0.0905	0.03	0.7391	0.26	CCC (13)+ τ CCCC (26)
80	416.28	1.3994	0.51	0.4867	0.17	CCC(10)
81	356.08	3.4298	1.24	0.97	0.34	ν SC (13)+ γ OCCS (34)
82	288.49	7.6971	2.78	7.535	2.64	ν CC(12)+ ϕCCC(16)+ ϕ CSC (10)
83	278.25	0.2447	0.09	1.9511	0.68	NCC (12)
84	262.16	8.8763	3.2	2.1066	0.74	OSC (12)+ ϕ CSC (27)
85	253.89	0.9119	0.33	4.3487	1.53	CCC (16)
86	244.82	5.7779	2.09	6.1194	2.15	ν SC (24)+ ϕ OSC(13)
87	209.05	12.2719	4.43	2.8247	0.99	γ OCCS(18)
88	191.53	2.689	0.97	5.2115	1.83	ν OC(13)+ τ CCSC(11)+ τ CSCC(11)+ γSCCC(12)
89	140.24	1.0201	0.37	0.7503	0.26	ν OC(19)+ ϕ CCC(13)+ γ SCCC(12)
90	110.24	1.4024	0.51	5.9412	2.08	SCC(10)+ τ CCCC(20)+ γ CCCC(10)
91	71.34	2.8913	1.04	1.1124	0.39	CCC (10)+ ϕ SCC(11)+E84
92	63.79	0.0301	0.01	5.6971	2	NCC (12)+ τ CSCC (29)+E84
93	54.54	1.7192	0.62	2.9169	1.02	ν OC(13)+ ν NC(10)+ ϕ OCN(11)+ τ CCCC(21)
94	43.57	0.0139	0.01	9.841	3.45	ν OC(10)+ ϕ CCC(11)+ τ CCCC(15)
95	36.82	0.3876	0.14	8.6392	3.03	ν CC(10)+ τ CCCC(27)
96	-664.12	0.7952	0.29	0.7893	0.28	ν CC (13)+ ϕ CCS(30)+ γOCNC(11)

ν-Stretching; ϕ-bending; γ-out-of-plane deformation; τ-torsion; potential energy distribution is given in brackets in the assignment column;

[a] Absolute IR and Raman intensity.

[b] Relative IR and Raman intensities normalized with highest peak absorption equal to 100.